OCEAN VECTOR WINDS IN STORMS FROM THE SMAP L-BAND RADIOMETER

Thomas Meissner, Lucrezia Ricciardulli, Frank Wentz

Remote Sensing Systems, 444 Tenth Street, Suite 200, Santa Rosa CA 95401, USA

Abstract

Our paper discusses the unique capability of the SMAP L-band radiometer to measure strong winds in tropical and extratropical cyclones. There is no significant degradation in rain.

INTRODUCTION AND OUTLINE

The Soil Moisture Active Passive Mission SMAP (Entekhabi et al., 2010) was launched in January 2015 and has been providing science data since April 2015. Though designed to measure soil moisture and despite the demise of its radar in July 2015, the SMAP sensor is very capable to measure ocean winds in storms at a resolution of 40 km. The L-band radiometer V-pol and H-pol channels keep excellent sensitivity to ocean surface wind speed even at very high wind speeds and they are only very little impacted by rain. The presence of polarimetric channels, which measure all 4 Stokes parameters on the SMAP radiometer, also allows retrieving wind direction.

We discuss the major features of the SMAP sensor, the geophysical model function that is used in the ocean vector wind retrieval and the basic steps of the retrieval algorithm. We then present a detailed validation of the SMAP wind fields in storms. The most important validation source is NOAA's airborne Step Frequency Microwave Radiometer SFMR, whose wind speeds were collocated with SMAP in space and time and resampled to its resolution. A comparison between SMAP and SFMR winds in one of the strongest hurricanes of the 2015 season shows excellent agreement up to 65 m/s and no degradation in rain. This gives SMAP a distinct advantage over many other space-borne sensors such as C-band or Ku-band scatterometers or radiometers, which either lose sensitivity at very high winds or degrade in rainy conditions.

THE SMAP L-BAND RADIOMETER

SMAP flies in a polar 8-day repeat orbit (98° inclination) at an average altitude of 685 km. It maps out a contiguous swath of approximately 1000 km width. The local times of the ascending/descending equatorial crossings are 18:00 and 6:00, respectively. The instrument has a mesh-antenna of 6-meter in diameter, which conically scans and takes observations over a full 360° scan at an average Earth incidence angle of 40°. The center frequency of the radiometer is 1.41 GHz. The calibration is performed internally through noise diode injection. The resolution of the instrument is about 40 km. SMAP is a fully polarimetric radiometer measuring vertical (V-pol) and horizontal (H-pol) polarizations as well as the 3rd (S3) and the 4th (S4) Stokes parameters, s, which describe the polarization state of the emitted radiation (Jackson, 1975) and are used for wind direction retrievals (Meissner and Wentz, 2006).

GEOPHYSICAL MODEL FUNCTION FOR THE WIND INDUCED SURFACE EMISSION

The geophysical model function (GMF) characterizes the change of the brightness temperature (TB) that is emitted from a rough ocean surface as function of surface wind speed. This is the basic signal that is used in retrieving ocean surface wind speeds from SMAP radiometer observation.

Our derivation of the SMAP L-band GMF is based on match-ups between SMAP TB and wind speeds from WindSat (Wentz et al., 2013), which is shown in Figure 1. The time window for the SMAP-WindSat match-ups is 1 hour and we require rain free scenes.
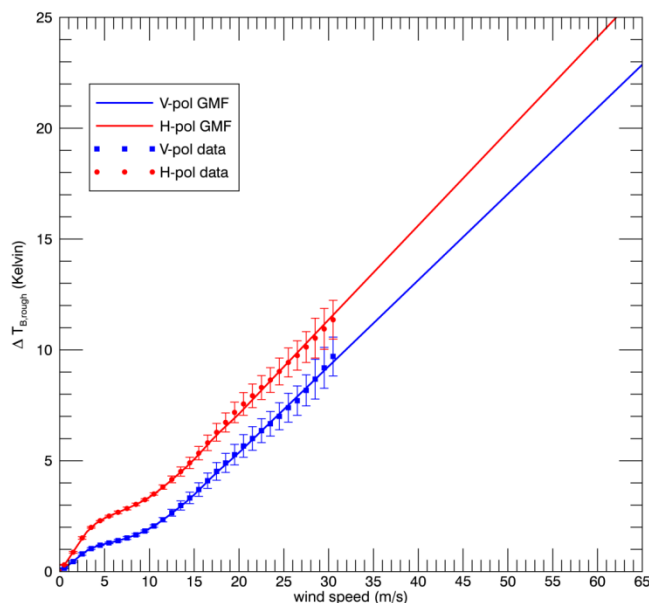

Figure 1: **SMAP wind induced surface brightness temperature for vertical (V-pol) and horizontal (H-pol) polarization as function of surface wind speed W. The symbols are the actual SMAP T_B measurements from the SMAP T_B – WindSat wind speed match-up data. The lines are the functional form of the GMF that were fitted to the data.**

The results indicate that the surface TB increases approximately linearly with wind speed above 18 m/s. At high winds, the microwave emission from wind roughened ocean surfaces is mainly caused by sea foam (Nordberg et al., 1971; Monahan and O'Muircheartaigh, 1980).   There are few valid SMAP – WindSat match-ups at wind speeds above 35 m/s. Based on the behaviour of the wind induced ocean surface emissivity at higher frequency (Meissner and Wentz, 2012) we linearly extrapolate the GMF above 35 m/s.

The derived SMAP GMF is in very good agreement with the one for the Aquarius L-band radiometer (Meissner et al., 2014). We have been using this GMF for the surface roughness correction in the SMAP ocean surface salinity retrieval algorithm (Meissner and Wentz, 2016).

WIND SPEED RETRIEVAL ALGORITHM

Figure 2 depicts schematically the basic steps of the SMAP wind speed retrieval algorithm. The inputs are SMAP L1B RFI-filtered antenna temperatures TA (Piepmeier et al., 2016), which are optimum interpolated onto a fixed 0.25 deg Earth grid. Several spurious signals have to be removed from the TA in order to obtain SMAP TB at the ocean surfaces. We follow the same steps as in the SMAP salinity retrievals (Meissner and Wentz, 2016).

We use ancillary input fields for salinity (www.hycom.org) and sea surface temperature (https://podaac.jpl. nasa.gov/dataset/CMC0.2deg-CMC-L4-GLOB-v2.0) and the sea water dielectric model of Meissner and Wentz (2004; 2012) to compute the emissivity of a flat ocean surface, which is subtracted from the measured SMAP TB. This isolates the wind induced signal which is matched to the GMF through a Maximum Likelihood Estimator (MLE). We use equal weights for V-pol and H-pol channels in the MLE.

Comparing the retrieved SMAP wind speeds with those from WindSat and NCEP (National Center for Environmental Prediction, www.nco.ncep.noaa.gov/pmb/products/gfs/) indicates an approximate global accuracy

of about 1.5 m/s for the SMAP winds. The dominant uncertainty source is radiometer noise. This is not as good as the global accuracy of wind speeds from many other spaceborne passive or active sensors (Wind-Sat, AMSR, SSMI, TMI, GMI, QuikScat, ASCAT). The major strength of the L-band radiometer is at high wind speeds (> 15 m/s), as it was first demonstrated for the SMOS (Soil Moisture and Ocean Salinity) mission (Reul et al., 2014).
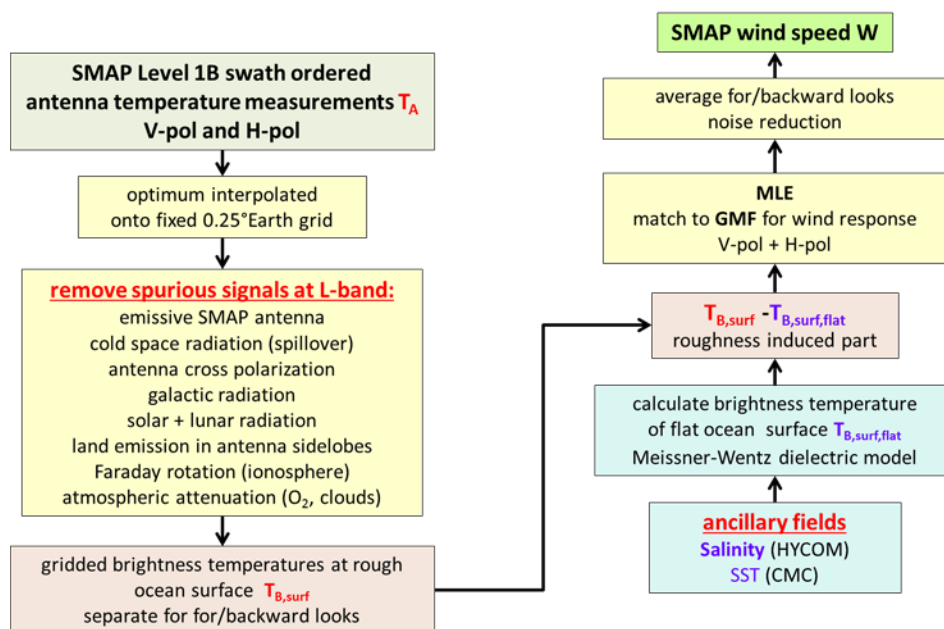

Figure 2: **Flow diagram for the SMAP wind speed retrieval algorithm.**

The SMAP wind speed retrieval algorithm does not depend on ancillary input wind fields from numerical weather prediction models.

VALIDATION: SMAP – SFMR

The SMAP wind retrievals at very high wind speeds are based on assuming that the GMF (Figure 1) can be linearly extrapolated above 35 m/s. We now verify this assumption by comparing the SMAP winds with an independent validation source that has not been used in developing the GMF.

The Stepped Frequency Microwave Radiometer (SFMR) (Uhlhorn et al., 2007) is flown regularly on hurricane penetrating aircrafts by NOAA and the US Air Force in tropical cyclones. The SFMR data are publicly distributed by NOAA's Hurricane Research Division (HRD) of the Atlantic Oceanographic and Meteorological Laboratory (AOML) [available at http://www.aoml.noaa.gov/hrd/data_sub/]. Klotz and Uhlhorn (2014) have developed an improved SFMR retrieval algorithm and shown that the SFMR wind speeds are in very good agreement with measurements from dropsondes. The dropsonde winds are regarded as ultimate ground truth but their coverage is too sparse in order to be used in validating satellite winds. The RMS (root mean square) difference between SFMR and dropsonde winds is about 3.9 m/s.

The resolution of the SFMR measurements is much finer than that of the SMAP footprint. In order to make a meaningful comparison between the measurements of the two instruments it is necessary to resample the SFMR observations from their fine resolution to the coarse SMAP resolution. The method for creating a SMAP – SFMR match-up is demonstrated in Figure 3 in the case of Hurricane Patricia (23 October 2015) as an example. Because of the time difference between the SMAP and SFMR overpasses (about 4 hours in this instance) it is also necessary to shift the SMAP wind speed field to the location of the SFMR track.
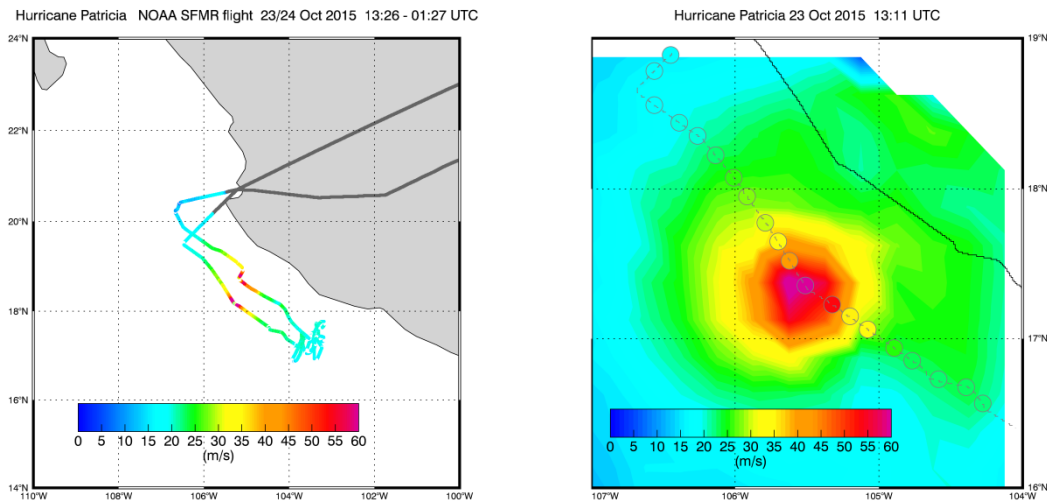
Figure 3: **SFMR flight segments through Hurricane Patricia on October 23rd, 2015 (left). In order to achieve a match-up between SMAP and SFMR (right), the lower SFMR segment (solid black line), which is closest in time to the SMAP overpass, is shifted so that the SFMR and SMAP storm centers coincide (dashed grey line). The SFMR wind speed observations are then averaged along-track into 0.25 deg boxes and compared with the SMAP wind speed cells (circles).**
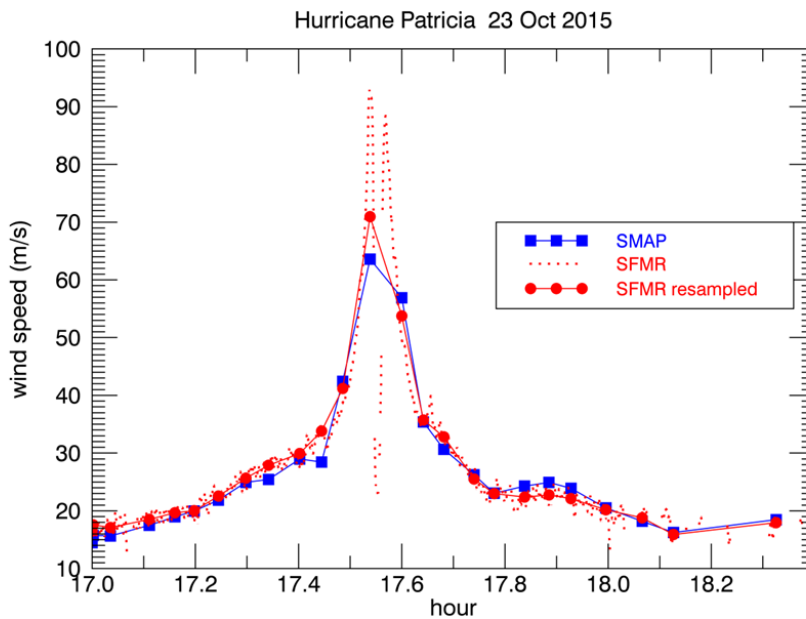

Figure 4: **Time series of the SMAP – SFMR matchups from Figure 3 along the SFMR track. The red dashed lines are the actual SFMR measurements. The red circles/solid lines show the SFMR measurements after averaging them along-track into 0.25 deg boxes. The time values of the x-axis refer to the SFMR flight.**

Figure 4 shows the time series of the cross section of the SMAP wind field along the SFMR track. SMAP and resampled SFMR wind speeds are in very good agreement along the whole track.

We were able to repeat the SMAP – SFMR match-up procedure for 10 tropical cyclones during 2015 for a total of 227 storm scenes. The resulting scatterplot (Figure 5) shows very good correlation and no significant systematic biases between the SMAP and the SFMR winds over a wide wind speed range of 15 – 65 m/s.

This validates the SMAP wind speed retrievals within a margin of error of about 10%. It also verifies the linear increase of the wind-induced L-band emissivity with wind speeds and thus proves that the L-band radiometer signal keeps good sensitivity to wind speed and does not saturate even at very high wind speeds.
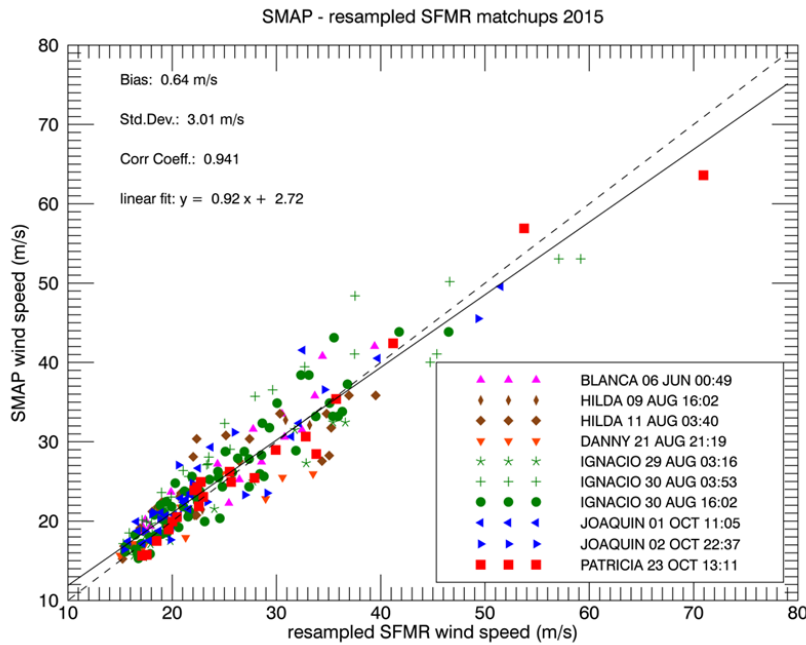

Figure 5: **Statistics of SMAP – resampled SFMR match-ups for 10 tropical cyclone overpasses during 2015. The linear regression fit is shown as solid black line and the perfect correlation is shown as dashed black line.**

DEGRADATION IN RAIN

It is well know that rain contamination constitutes a large if not prohibitive problem to measure wind speeds with microwave radiometers at higher frequencies and to a lesser extent also at Ku-band scatterometers. For C-band scatterometers heavy rain causes moderate degradation in the measured wind speeds. In addition to the good sensitivity at high wind speeds, another advantage of the L-band radiometers for measuring wind speeds in storms is that it is basically unaffected by rain. The atmospheric attenuation is negligible at L-band frequencies even at high rain rates.

As the SFMR is also able to measure rain, this can also be demonstrated from the SMAP – SFMR match-up data set. Table 1 shows the wind speed statistics stratified as function of rain rate. There is no systematic degradation with increasing rain rate.

Resampled SFMR Rain Rate (mm/ h)	# of match-ups	Bias SMAP – SFMR wind speed (m/s)	Std. Dev. SMAP – SFMR wind speed (m/s)
0 – 5	136	0.68	2.55
5 - 10	52	1.57	3.37
10 - 15	19	0.46	2.85
> 15	20	-1.86	3.69

Table 1: **Statistics of SMAP – resampled SFMR match-ups for different rain rates. The SFMR rain rate has been averaged to 0.25 deg.**
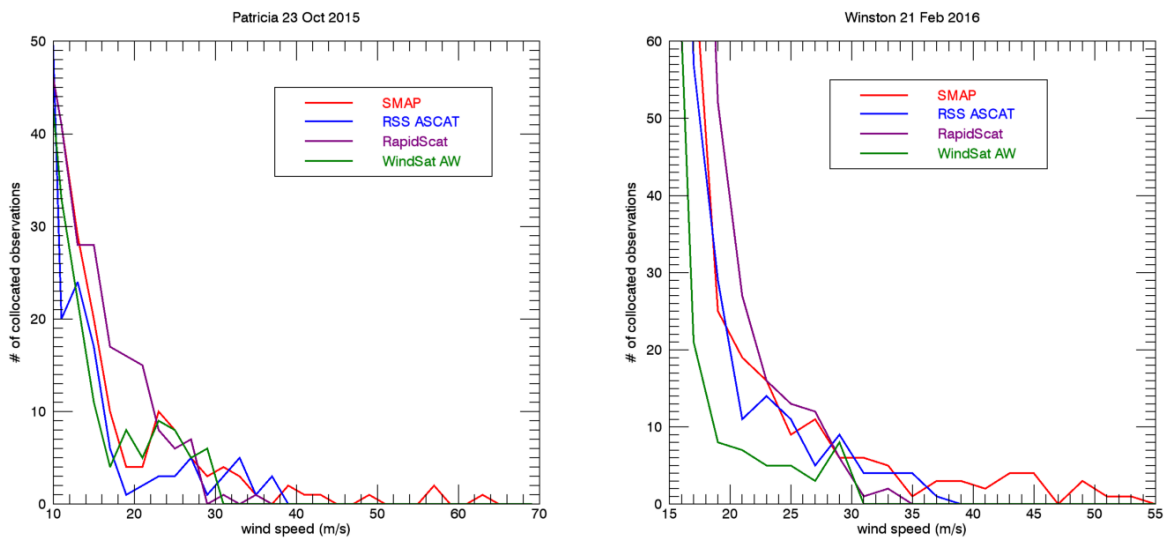
COMPARISON WITH OTHER SPACEBORNE SENSORS

Figure 6: Collocated histograms of wind speed distributions of SMAP, RSS ASCAT (Ricciardulli and Wentz, 2017), RapidScat (http://dx.doi.org/10.5067/RSX12-L2B11) and the RSS WindSat All-Weather winds (Meissner and Wentz, 2009). The bin size is 2 m/s. The histograms in the figures count only wind cells in a 0.25 deg grid for which all four sensors have valid observations. Left: Hurricane Patricia on October 23rd, 2015. From all four sensors, only SMAP exceeds 36 m/s reaching a maximum of 64 m/s. Right: Hurricane Winston on February 21st, 2016. From all four sensors, only SMAP exceeds 36 m/s reaching a maximum of 53 m/s.

Figure 6 shows a comparison of collocated wind speed distributions of SMAP and several other sensors in Hurricanes Patricia and Winston. From the four sensors only SMAP is able to see wind speeds above 36 m/s. The RSS WindSat all weather winds were trained by a statistical algorithm in order to mitigate the rain impact and the training set did not contain a sufficient wind speed population above 40 m/s. The scatterometers (ASCAT, RapidScat) show signs of a saturating signal at very high wind speeds. In addition, the Ku-band scatterometer (RapidScat) is also strongly affected by rain.

NEAR REAL TIME PROCESSING

A BETA version of SMAP wind speeds is processed in near real time at Remote Sensing Systems. A daily Level 3 product is available in netCDF4 format at www.remss.com/missions/smap (Figure 7).
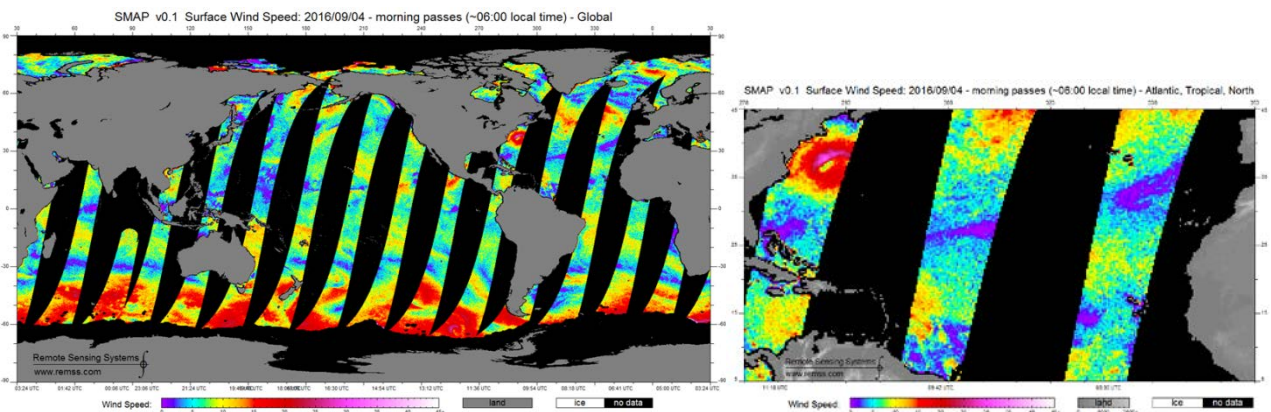

Figure 7: Snapshot of SMAP wind processing at the RSS website www.remss.com/smap.

Data are available starting April 1, 2015 until current with an average latency of about 7 hours.

WIND DIRECTION RETRIEVALS

Because of its polarimetric channels (3rd and 4th Stokes parameters) SMAP has also limited capability to measure wind direction at wind speeds above 15 m/s. In order to reduce the noise it is necessary to decrease the spatial resolution to about 100 km and thus is only useful in large extratropical cyclones.

CONCLUSION

L-band satellite radiometers allow measuring the intensity of tropical and extratropical storms. The reason is that the wind-induced surface emission at L-band increases approximately linearly with wind speed between 18 and 65 m/s and shows no signs of saturation at any wind speeds nor is it significantly affected by rain. This provides a distinct advantage over many other active and passive space-borne sensors, whose signal saturates in high winds or which degrade in rain. The spatial resolutions of spaceborne passive L-band sensors that are currently operating (SMOS and SMAP) are limited to about 40 km.

REFERENCES

Entekhabi, D., and Coauthors, (2010) The Soil Moisture Active Passive (SMAP) Mission. Proc. IEEE, **98**(5), pp 704-716, doi: 10.1109/JPROC.2010.2043918.

Jackson, J. D., (1975) Classical Electrodynamics, John Wiley & Sons, New York.

Klotz, B., and E. Uhlhorn, (2014) Improved stepped frequency microwave radiometer tropical cyclone surface winds in heavy precipitation. J. Atmos. Ocean. Tech., **31**, pp 2392- 2408, doi: 10.1175/JTECH-D-14-00028.1.

Meissner, T., and F. Wentz, (2004) The complex dielectric constant of pure and sea water from microwave satellite observations. IEEE Trans. Geosci. Rem. Sens., **42**(9), pp 1836-1849, doi: 10.1109/TGRS.2004.831888.

Meissner, T., and F. Wentz, (2006) Ocean Retrievals for WindSat: Radiative transfer model, algorithm, validation. Presentation at the *9th Specialist Meeting on Microwave Radiometry and Remote Sensing Applications*, San Juan, Puerto Rico, USA, IEEE Catalog no. 06EX1174C, doi: 10.1109/MICRAD.2006.1677074.

Meissner, T., and F. Wentz, (2009) Wind vector retrievals under rain with passive satellite microwave radiometers. IEEE Trans. Geosci. Rem. Sens., **47**(9), pp 3065-3083 doi: 10.1109/TGRS.2009.2027012.

Meissner, T., and F. Wentz, (2012) The emissivity of the ocean surface between 6 - 90 GHz over a large range of wind speeds and Earth incidence angles. IEEE Trans. Geosci. Rem. Sens., **50**(8), pp 3004-3026, doi: 10.1109/TGRS.2011.2179662.

Meissner, T., F. Wentz, and L. Ricciardulli, (2014) The emission and scattering of L-band microwave radiation from rough ocean surfaces and wind speed measurements from the Aquarius sensor. J. Geophys. Res., **119,** doi: 10.1002/2014JC009837.

Meissner, T. and F. Wentz, (2016) Remote Sensing Systems SMAP Ocean Surface Salinities Level 2C, Version 2.0 validated release. Remote Sensing Systems, Santa Rosa, CA, USA. Available online at www.remss.com/missions/smap, doi: 10.5067/SMP20-2SOCS.

Monahan, E., and I. O'Muircheartaigh, (1980) Optimal power-law description of oceanic white-cap coverage dependence on wind speed, J. Phys. Oceanogr., **10**, pp 2094-2099, doi: 10.1175/1520-0485(1980)010 <2094:OPLDOO>2.0.CO;2.

Nordberg, W., J. Conaway, D. Ross, and T. Wilheit, (1971) Measurement of microwave emission from a foam covered wind driven sea, J. Atmos. Sci., **38**, pp 429-433, doi: http://dx.doi.org/10.1175/1520-0469(1971)028<0429:MOMEFA>2.0.CO;2.

Piepmeier, J. R., P. Mohammed, J. Peng, E. J. Kim, G. De Amici, and C. Ruf, (2016) SMAP L1B Radiometer Half-Orbit Time-Ordered Brightness Temperatures, Version 3. CRID 13080. [RFI filtered antenna temperatures]. Boulder, Colorado USA. NASA National Snow and Ice Data Center Distributed Active Archive Center. http://dx.doi.org/10.5067/YV5VOWY5V446.

Reul, N., J. Tenerelli, B. Chapron, D. Vandemark, Y. Quilfen, and Y. Kerr, (2012) SMOS satellite L-band radiometer: A new capability for ocean surface remote sensing in hurricanes. J. Geophys. Res., **117**, C02006, doi: 10.1029/2011JC007474.

Ricciardulli, L., and F. Wentz, (2016) Remote Sensing Systems ASCAT C-2015 Daily Ocean Vector Winds on 0.25 deg grid, Version 02.1. Remote Systems, Santa Rosa, CA. Available online at www.remss.com/missions/ascat.

Uhlhorn, E., J. Franklin, M. Goodberlet, J. Carswell, and A. Goldstein, (2007) Hurricane surface wind measurements from an operational stepped frequency microwave radiometer. Mon. Wea. Rev., **135**(9), 3070 – 3085, doi: http://dx.doi.org/10.1175/MWR3454.1.

Wentz, F., L. Ricciardulli, C. Gentemann, T. Meissner, K. Hilburn, and J. Scott, (2013) Remote Sensing Systems Coriolis WindSat Daily Environmental Suite on 0.25deg grid, Version 7.0.1 LF Wind Speeds. Remote Sensing Systems, Santa Rosa, CA. Available online at www.remss.com/missions/windsat.